Nanomanufacturing and Metrology (2018) 1:217–224
https://doi.org/10.1007/s41871-018-0023-x

ORIGINAL ARTICLES

Surface Flattening and Nanostructuring of Steel by Picosecond Pulsed Laser Irradiation

Tomoki Kobayashi[1] · Hiroshi Sera[2] · Tomohiro Wakabayashi[2] · Haruyuki Endo[3] · Yuichi Takushima[3] · Jiwang Yan[1]

Received: 5 July 2018 / Revised: 21 August 2018 / Accepted: 28 August 2018 / Published online: 5 September 2018

Abstract
Steel is used as a mold material for press/injection molding of plastic products. High accuracy and releasing ability are required for a steel mold surface. This paper proposes a surface finishing method for steel molds by using picosecond pulsed laser irradiation. The process involves two steps: one is surface flattening by removing the surface asperity through laser ablation, and the other is forming nanoscale laser-induced periodic surface structures (LIPSS) on the flattened surface. The two steps are realized by using the same laser at controlled laser fluence and focus position. Experimental results showed that LIPSS was successfully formed after surface flattening under specific ranges of laser fluence and defocus length. Furthermore, plastic forming experiments demonstrated that a steel surface with LIPSS significantly decreased the effective contact area and, in turn, reduced the mold releasing force. These findings provide the possibility of fabricating high-performance steel molds by picosecond pulsed laser irradiation.

Keywords Surface flattening · Nanostructure · Steel material · Picosecond pulsed laser · Plastic molding · Mold releasing ability

1 Introduction

In modern industry, various kinds of plastic products are produced by press molding and injection molding processes. In high-precision molding technologies, it is important that the surface of a mold has high accuracy because the accuracy of the mold directly affects the accuracy of the resulting plastic products. At the same time, high mold releasing ability is also necessary to prevent adhesion of plastic onto the mold.

Conventionally, mechanical polishing has been used to improve the surface quality and modify the form error of a mold. However, polishing becomes difficult when the mold surface feature is smaller than millimeter size and its shape is complicated. To solve this problem, laser polishing of a mold has been attempted [1]. In laser polishing, a layer of mold material is melted by laser irradiation and the surface becomes flat due to the surface tension effect. Laser polishing can improve surface roughness without deforming the surface shape [2]. However, the heat-affected zone in the laser-polished mold is very thick (∼ tens of microns) because a thick layer of material is melted [3, 4]. The heat-affected zone might reduce the strength and, in turn, the service life of a mold.

On the other hand, during plastic molding, a releasing agent is necessary to prevent plastic from sticking to the mold surface. However, it is difficult to apply the releasing agent uniformly on a small mold with complicated surface geometry. The releasing agent, even uniformly applied, may be damaged and even peeled off after molding. As a result, it is necessary to apply the releasing agent repeatedly, which significantly reduces the production efficiency.

In this study, the authors propose a surface finishing method for a steel mold by picosecond pulsed laser

✉ Jiwang Yan
yan@mech.keio.ac.jp

[1] Department of Mechanical Engineering, Keio University, Hiyoshi 3-14-1 Kohoku, Yokohama, Kanagawa 223-8522, Japan

[2] Yazaki Corporation, Hikarinooka 3-1, Yokosuka, Kanagawa 239-0847, Japan

[3] Optoquest Co., Ltd, Haraiti 1335, Ageo, Saitama 362-0021, Japan

irradiation. The method involves two steps: the first is surface flattening by removing the surface asperities through laser ablation, and the second is forming nanoscale laser-induced periodic surface structures (LIPSS) on the flattened surface. In recent years, the ultrashort pulse laser has been extensively investigated, and it has been demonstrated that irradiating ultrashort pulse laser can significantly decrease the thickness of heat-affected zones [5]. Previous studies have focused on ultrashort pulse laser irradiation to form fine patterns or clean holes [6–8]. However, there is very few research on surface flattening using ultrashort pulse laser ablation. LIPSS formation has also been focused for various materials at femtosecond pulses [9–12]. It is known that the period of LIPSS depends on the laser wavelength [13, 14], and its orientation and shape are defined by the polarization of incident laser [10, 15]. A lot of researches have been carried out to investigate the physics underlying the formation of LIPSS for different materials [13, 16–18]. Although the formation mechanism of LIPSS is still under investigation at the moment, LIPSS has been widely utilized to improve surface properties, such as wettability [19–21], optical performance [22, 23], and tribology [24].

In this study, picosecond pulsed laser irradiation was performed on steel to realize surface flattening and to form LIPSS on the flattened surface. It is expected that the LIPSS can improve the mold releasing ability of a steel mold and reduce the necessity for applying releasing agent. Surface flattening and LIPSS formation will be combined into a single process by using a single laser beam. This study can improve both surface accuracy and releasing ability of steel molds, thus contributing to the high-precision micro-/nanomanufacturing industry.

2 Mechanism of Surface Flattening and LIPSS Generation for Steel

Figure 1 shows the mechanism of surface flattening by laser irradiation. There is an energy density distribution within the laser beam in the direction of beam propagation where the fluence decreases with an increase in distance from the focal point, as shown in Fig. 1a. While the fluence of the elliptical region is higher than the ablation threshold, laser ablation arises. Consequently, the material removal only occurs in this elliptical region, and the surface asperity is removed preferentially within this region. During the laser scanning along a surface, the amount of material removal is larger near the center of the elliptical region than in the outer regions. Due to this difference, surface protrusions are selectively removed, and the bottom regions of depressions are less affected, as shown in Fig. 1b. In this way, the surface becomes flatter by

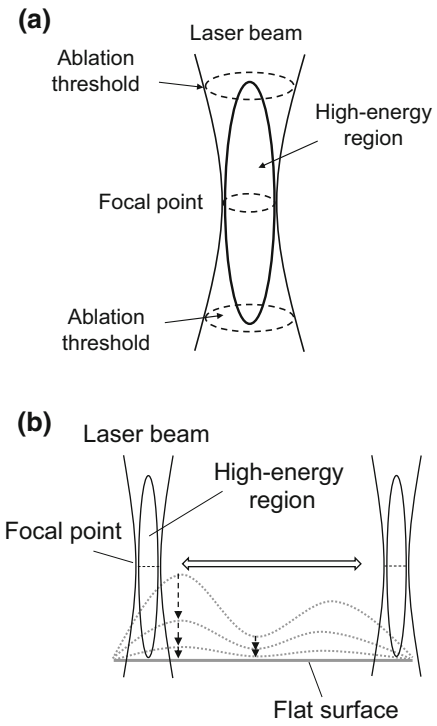

Fig. 1 Mechanism of surface flattening: **a** energy density distribution within a laser beam, **b** change in material removal amount with defocusing

scanning the laser beam repeatedly, without the need for melting the surface layer.

After surface flattening removes the surface asperities, LIPSS is formed on the flat surface by scanning the surface using the region just below the ablation threshold, as shown in Fig. 2a. The LIPSS formation for metal materials might be based on two different mechanisms. The one is the interference of laser and the surface plasmon polariton (SPP) excited by the ultrashort pulse laser [13, 16]. As shown in Fig. 2b, due to laser irradiation, an electric charge distribution is generated on the surface. This distribution induces electromagnetic field wave, i.e., SPP. LIPSS is a result of ablation on the modulated energy deposition caused by interference of incident laser and SPP. The other mechanism is laser-induced material self-organization [17]. As shown in Fig. 2c, the emission of electrons caused by absorbing laser induces instability in the surface, and the lattice is perturbed. As a result, LIPSS is assembled by surface relaxation due to the instability of surface. In the case of steel, it was shown that the mechanism of LIPSS formation was due to self-organization [17]. Under this condition, LIPSS is formed on the surface, and very little material is removed.

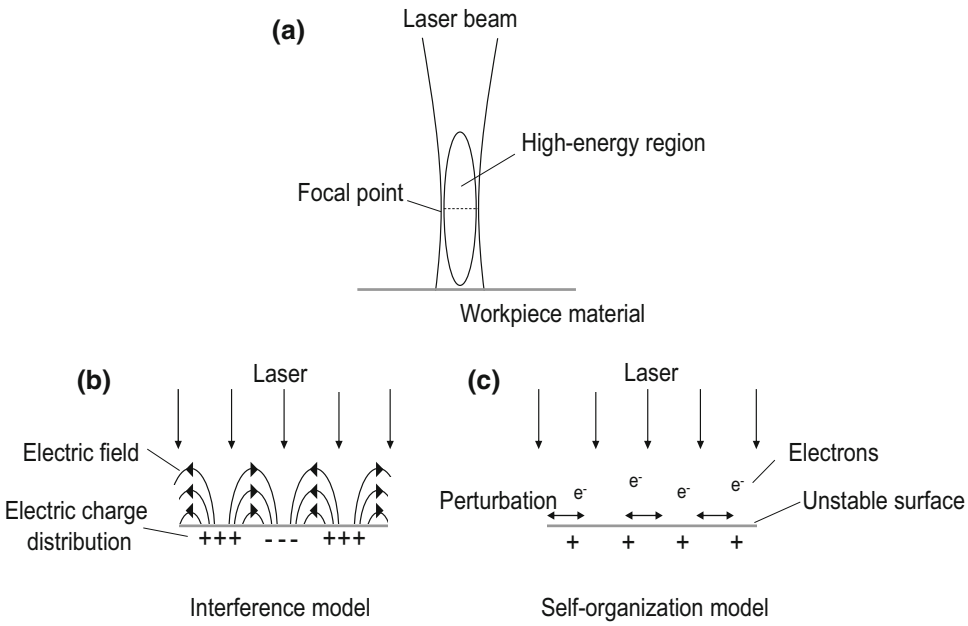

Fig. 2 Schematic of LIPSS generation after surface flattening

3 Experimental Methods

3.1 Ablation Threshold/Surface Flattening/ Nanostructuring

The laser used in the following experiments was PFLA-1030TP, an Yb fiber laser, produced by Optoquest Co., Ltd. The wavelength was 1030 nm. The pulse width was 50 ps, and the repetition frequency was 100 kHz. The energy density of the laser beam had a Gaussian distribution. Fluence was changed in 0.12–4.5 J/cm^2. The laser beam was focused into an elliptical spot with a size of 6 × 7 μm. (The focal length was 20 mm.) A stage was used to move the workpiece in the *X*-, *Y*- and *Z*-axis directions. A CCD camera and a lens were embedded vertically to set the focal point at the same height, as shown in Fig. 3. The focal point of the laser was adjusted on the sample surface by moving the stage in *Z*-axis. This was done, while the surface was being observed with the CCD camera during the adjustment. The number of pulses was 100 in a spot irradiation. The scanning speed was 40 mm/s with scan overlap (2 μm), and the number of irradiations was 15 and 50 in area irradiation. As workpiece, a stainless tool steel consisting of C (0.38%), Si (0.9%), Mn (0.5%), Cr (13.6%),V (0.3%), with a smooth surface, was used for finding ablation threshold and a rough cut surface was used for flattening surface (0.94 μm Ra). The defocus length was defined as 0 when the focal point was on the top of the surface asperity. The defocus length was changed from 0 to 40 μm to measure the size of the high-energy elliptical region for ablation. Debris generated during laser irradiation were removed by blowing Ar gas.

The resulting surface was observed by a scanning electron microscope (SEM), INSPECT S50 produced by FEI Company. The depth of the irradiated area was measured by a laser-probe profilometer, NH-3SP produced by

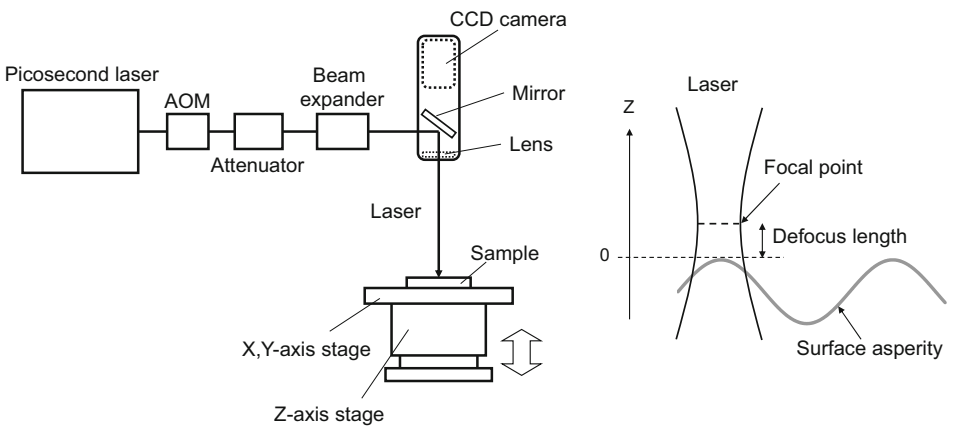

Fig. 3 Schematic of the experimental setup

Mitaka Kohki Co., Ltd. The depth of spot and the surface roughness of irradiated area were measured by a laser microscope, VK-9700 produced by KEYENCE CORPORATION.

3.2 Releasing Ability Evaluation

After laser processing of steel mold surfaces, the samples were used to evaluate the releasing force by press molding experiment. The pressed area of the sample was 8 mm × 8 mm. Polybutylene terephthalate (PBT) was pressed on the steel sample surface by a high-precision molding machine GMP211 produced by Toshiba Machine Co., Ltd. Molding temperature was 230 °C, near the melting point of the PBT plastic (224 °C). Pressing time was 20 s, and pressing force was 0.2 kN. Releasing force was calculated from the load which was used to separate the PBT sample from the stainless tool steel.

4 Results and Discussion

4.1 Ablation Threshold

In order to find the ablation threshold, laser pulses ($N = 100$) were irradiated onto a single spot changing fluence within the range of 0.12–4.5 J/cm^2, and the focal point was set to the sample surface. The relationship between the fluence and ablation rate is plotted in Fig. 4. The ablation rate is the spot depth per laser pulse. Further, the ablation threshold is defined as the fluence where the ablation rate sharply decreased [25]. In this case, due to the sharp decline of the ablation rate at 0.20 J/cm^2, the ablation threshold was around this fluence.

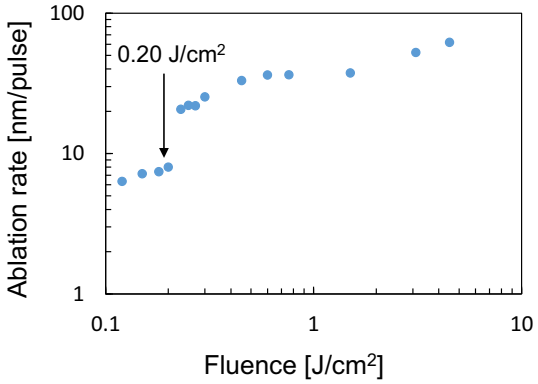

Fig. 4 Relationship between the fluence and ablation rate

4.2 Effect of Laser Fluence on Surface Morphology

In order to find the effect of laser fluence on surface morphology, laser fluence was changed in the range of 0.15–4.5 J/cm^2, and the defocus length was set to 0. (The focal point was set to the top of asperity.) The laser irradiation was performed for 15 passes. The SEM images of surfaces irradiated at various laser fluence are shown in Fig. 5. At the fluence of 0.15 J/cm^2, low spatial frequency LIPSS (LSFL) [26] with a period of ∼ 1 μm, which is close to the laser wavelength, was formed on the surface. At 0.76 J/cm^2, the only shallow structure was confirmed at one side of the irradiated line. When the fluence was 3.1 J/cm^2, no LIPSS was found. Instead, there were overlaps of the molten layers on the surface. The difference in surface morphology with changing fluence was caused by the difference in the amount of heat generated inside the material. When the fluence is low, near the ablation threshold, there is almost no thermal effect because the amount of heat generation is very small. As a result, LIPSS forms on the surface. On the other hand, thermal effect causes melting and material removal in a wide range at higher fluence [27]. As shown in Fig. 5d, the surface layer of workpiece material melted and spread by flowing while the material was partially removed.

4.3 Effect of Defocus Length on Surface Morphology

In order to find the effect of defocusing for surface flattening and nanostructuring, the defocus length was changed from 0 to 40 μm, and laser fluence was set to 0.76 J/cm^2. The laser irradiation was performed for 50 passes to remove surface asperity. The SEM image of the original surface is shown in Fig. 6. The SEM images of the surfaces irradiated at each defocus length are shown in Fig. 7. When the defocus length was 0, shallow LIPSS was formed at one side of the irradiated line, while no LIPSS was found at the center of the line (Fig. 7a). As the defocus length became 10 and 26 μm, LSFL was formed steadily on the surface (Fig. 7b, c). When the defocus length became 40 μm, however, high spatial frequency LIPSS (HSFL) [28, 29] was formed on the surface (Fig. 7d). It is known that HSFL is formed at lower fluence as compared with LSFL, and the period is significantly smaller than the laser wavelength [28]. This change in the surface morphology might have been caused by the expansion of the laser beam due to defocusing. When the beam is focused on the surface, the spot size is small with higher fluence, and material in the center of the spot is melted. As the beam radius was expanded by defocusing, the fluence decreased near the

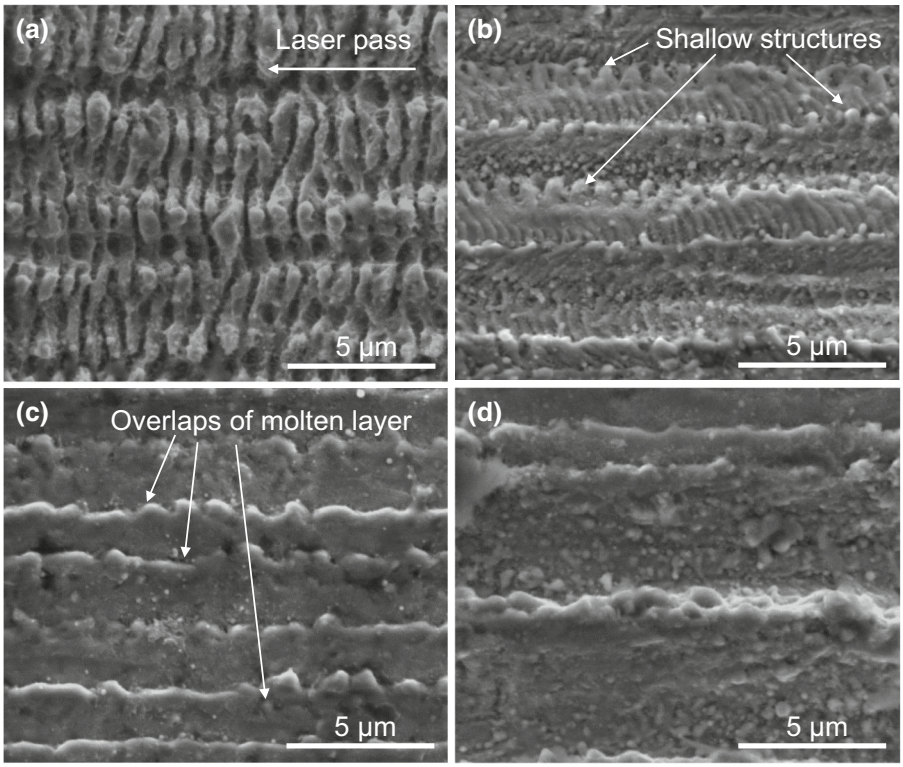

Fig. 5 SEM images of stainless tool steel surfaces irradiated at laser fluence of **a** 0.15, **b** 0.76, **c** 3.1, **d** 4.5 J/cm^2

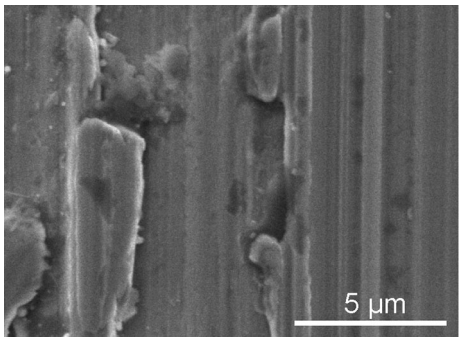

Fig. 6 SEM image of original stainless steel surface

ablation threshold, and thus LSFL was formed on the surface. When the defocus length was further increased ($\sim$ 40 μm), LSFL was not observed, and instead, HSFL was created, because in this case, the fluence was significantly lower than the ablation threshold.

4.4 Effect of Defocusing on Material Removal Amount and Surface Roughness

The surface profiles of irradiated areas at each defocus length are shown in Fig. 8. This profile was measured in parallel with cutting tool marks. It is observed that the material removal amount decreased with the increase in the defocus length, and material was hardly removed when the defocus length was 40 μm. The change in material removal amount was dependent on the relationship between the defocus length and the high-energy elliptical region. Material removal occurs if the defocus length is smaller than the size of the high-energy elliptical region. When the defocus length was further increased ($\sim$ 40 μm), the material was hardly removed.

Then, fluence with defocusing laser was calculated. When the laser beam has a Gaussian distribution, the beam radius at the defocused position $w_{(z)}$ is calculated by

$$w_{(z)} = w_0\sqrt{1+\frac{z^2\lambda^2}{\pi^2 w_0^4}} \tag{1}$$

where w_0 is the beam radius at the focal point and λ is the wavelength. Laser fluence F is calculated by

$$F = \frac{P_{\text{ave}}/f}{\pi w_{(z)}^2} \tag{2}$$

where P_{ave} is the average laser power and f is the frequency of laser pulse. Fluence is changed with defocusing when P_{ave} is constant. By using Eqs. (1) and (2), defocus length where fluence became around 0.20 J/cm^2 which was defined as the ablation threshold in Fig. 4 was calculated as 45 μm. This calculated result was close to the experimental result of the high-energy elliptical region (40 μm).

The change in surface roughness with defocusing is shown in Fig. 9. Compared with the original cut surface (0.94 μm Ra), the surface roughness was improved by laser

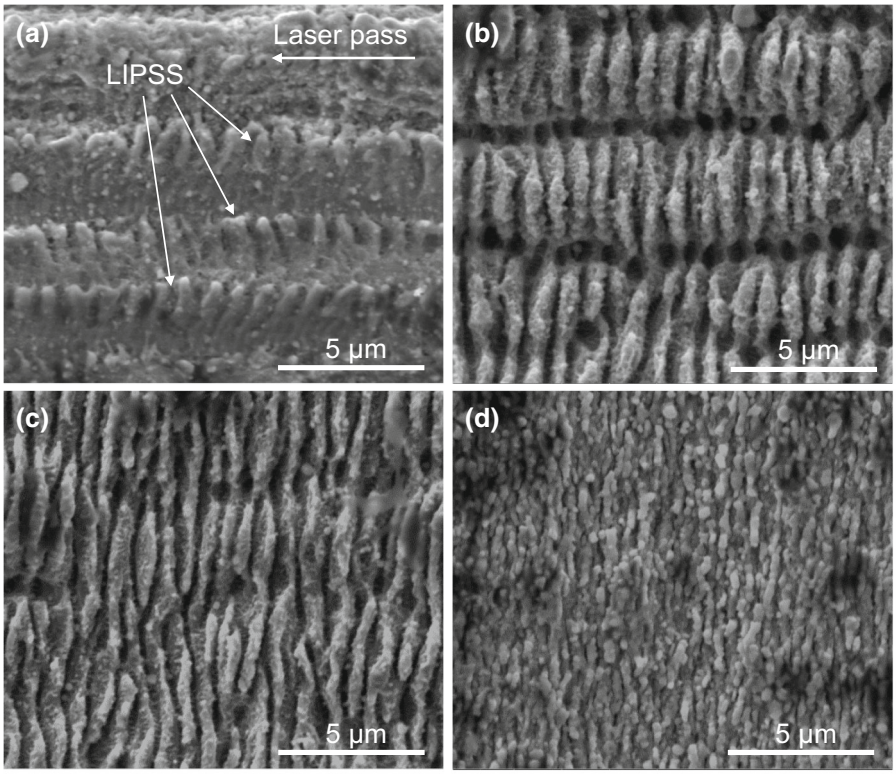

Fig. 7 SEM images of stainless tool steel surfaces irradiated at defocus length of **a** 0 μm, **b** 10 μm, **c** 26 μm, **d** 40 μm

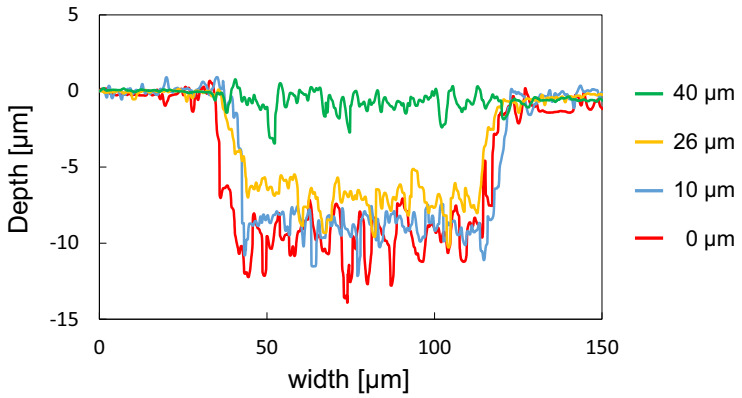

Fig. 8 Surface profiles of irradiated areas at each defocus length

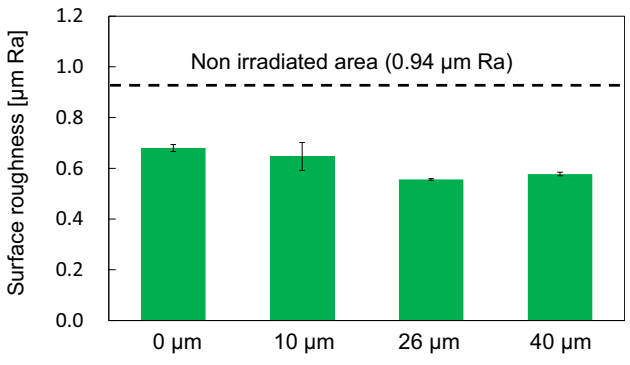

Fig. 9 Change in surface roughness with defocusing

irradiation. In particular, when the defocus length was set to 26 μm, the surface roughness was improved to 0.56 μm Ra. The formation of nanoscale LIPSS did not cause surface roughness to increase.

4.5 Surface Releasing Ability

Figure 10 shows the SEM images of the irradiated surface of a steel mold before and after plastic press molding. LIPSS was formed on the smooth surface. After molding, the surface remained unchanged, and the plastic did not enter the nanoscale grooves of LIPSS during molding. Figure 11 shows the SEM image of the pressed plastic

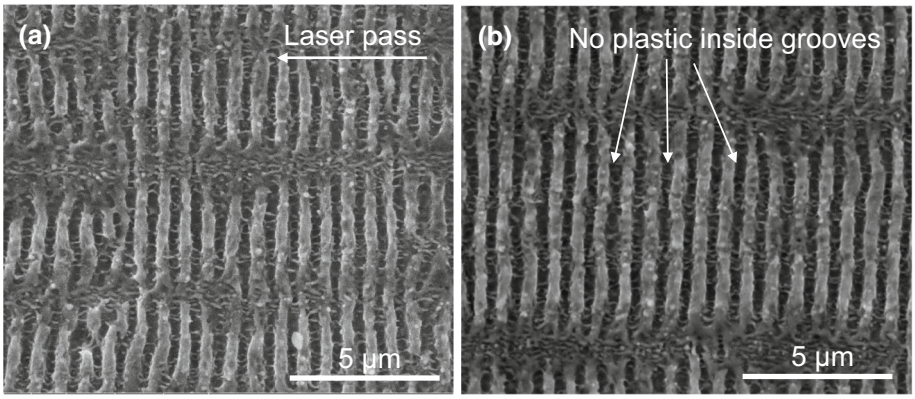

Fig. 10 SEM images of steel mold surface **a** before and **b** after press molding

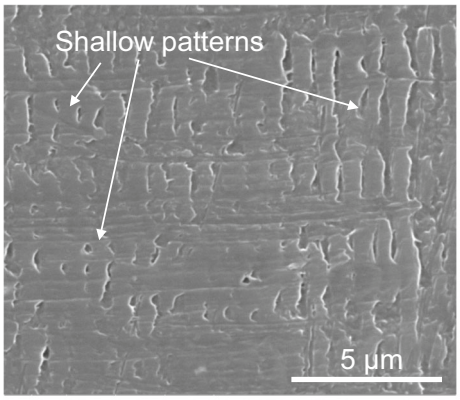

Fig. 11 SEM image of PBT surface after press molding

surface. There were very slight imprinting patterns on the plastic surface, but they were extremely shallow.

Figure 12 shows the releasing force between the plastic and the steel molds under different conditions. Forming LIPSS on the mold surface decreased the releasing force by a factor of three. This might be due to the decrease in effective contact area after forming LIPSS on the mold surface, as schematically shown in Fig. 13. In particular, in this experiment, pressing temperature was set around the

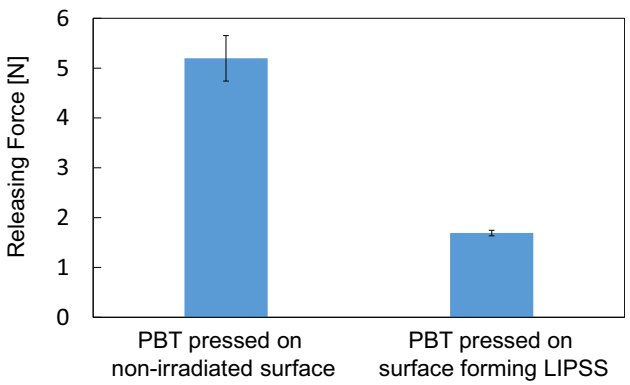

Fig. 12 Releasing force between PBT and steel mold with/without laser processing

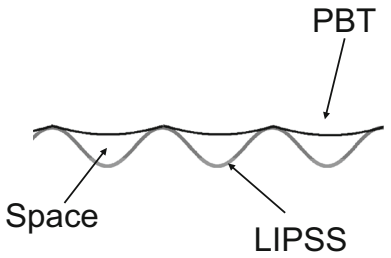

Fig. 13 Schematic of the contact area of LIPSS and PBT

melting point of the plastic, at which the viscosity of plastic was still high, making it difficult to fill the nanoscale grooves [30]. Therefore, forming LIPSS on the steel mold surface improved the mold releasing ability.

5 Conclusions

Picosecond pulsed laser was irradiated on steel mold surfaces at controlled laser fluence and focus position, and laser-induced surface flattening and formation of LIPSS were investigated. After surface flattening by ablation at a higher laser fluence, LIPSS was successfully formed on the surface with a low surface roughness (0.56 μm Ra) at a specific defocus length. Forming LIPSS on a steel mold surface decreased the effective contact area during plastic molding, and the mold releasing force was decreased by a factor of three. The findings from this study demonstrated the possibility of improving surface flatness and releasing ability of steel molds by irradiating a picosecond pulsed laser.

References

1. Pfefferkorn FE, Duffie NA, Li X, Vadali M, Ma C (2013) Improving surface finish in pulsed laser micro polishing using thermocapillary flow, CIRP. Ann-Manuf Technol 62:203–206

2. Lamikiz A, Sánchez JA, López de Lacalle LN, Arana JL (2007) Laser polishing of parts built up by selective laser sintering. Int J Mach Tool Manuf 47:2040–2050
3. Schmidt J, Scholz R, Riegel H (2015) Laser polishing of aluminum by remelting with high energy pulses. Materialwiss Werksttech 46:686–691
4. Ukar E, Lamikiz A, López de Lacalle LN, del Pozo D, Arana JL (2010) Laser polishing of tool steel with CO_2 laser and high-power diode laser. Int J Mach Tool Manuf 50:115–125
5. Chichkov BN, Momma C, Nolte S, von Alevensleben F, Tiinnermann A (1996) Femtosecond, picosecond and nanosecond laser ablation of solids. Appl Phys A 63:109–115
6. Borowiec A, Haugen HK (2004) Femtosecond laser micromachining of grooves in indium phosphide. Appl Phys A 79:521–529
7. Crawford THR, Borowiec A, Haugen HK (2005) Femtosecond laser micromachining of grooves in silicon with 800 nm pulses. Appl Phys A 80:1717–1724
8. Kamlage G, Bauer T, Ostendorf A, Chichkov BN (2003) Deep drilling of metals by femtosecond laser pulses. Appl Phys A 77:307–310
9. Vorobyev AY, Makin VS, Guo C (2007) Periodic ordering of random surface nanostructures induced by femtosecond laser pulses on metals. J Appl Phys 101:034903
10. Bonse J, Krüger J, Höhm S, Rosenfeld A (2012) Femtosecond laser-induced periodic surface structures. J Laser Appl 24:042006
11. Tomita T, Kinoshita K, Matsuo S, Hashimoto S (2007) Effect of surface roughening on femtosecond laser-induced ripple structures. Appl Phys Lett 90:153115
12. Vorobyev AY, Guo C (2007) Femtosecond laser structuring of titanium implants. Appl Surf Sci 253:7272–7280
13. Albu C, Dinescu A, Filipescu M, Ulmeanu M, Zamfirescu M (2013) Periodical structures induced by femtosecond laser on metals in air and liquid environments. Appl Surf Sci 278:347–351
14. Vorobyev AY, Guo C (2008) Femtosecond laser-induced periodic surface structure formation on tungsten. J Appl Phys 104:063523
15. Reif J, Varlamova O, Costache F (2008) Femtosecond laser induced nanostructure formation: self-organization control parameters. Appl Phys A 92:1019–1024
16. Sakabe S, Hashida M, Tokita S, Namba S, Okamuro K (2009) Mechanism for self-formation of periodic grating structures on a metal surface by a femtosecond laser pulse. Phys Rev B 79:033409
17. Gregorčič P, Sedlaček M, Podgornik B, Reif J (2016) Formation of laser-induced periodic surface structures (LIPSS) on tool steel by multiple picosecond laser pulses of different polarizations. Appl Surf Sci 387:698–706
18. Martens JR, Uhlig S, Ratzke M, Varlamova O, Valette S, Benayoun S (2015) On large area LIPSS coverage by multiple pulses. Appl Surf Sci 336:249–254
19. Zhang Y, Zou G, Liu L, Zhao Y, Liang Q, Wu A, Zhou YN (2016) Time-dependent wettability of nano-patterned surfaces fabricated by femtosecond laser with high efficiency. Appl Surf Sci 389:554–559
20. Calderon MM, Rodríguez A, Ponte AD, Miñana MCM, Aranzadi MG, Olaizola SM (2016) Femtosecond laser fabrication of highly hydrophobic stainless steel surface with hierarchical structures fabricated by combining ordered microstructures and LIPSS. Appl Surf Sci 374:81–89
21. Wu B, Zhou M, Li J, Ye X, Li G, Cai L (2009) Superhydrophobic surfaces fabricated by microstructuring of stainless steel using a femtosecond laser. Appl Surf Sci 256:61–66
22. Vorobyev AY, Guo C (2008) Colorizing metals with femtosecond laser pulses. Appl Phys Lett 92:041914
23. Yao J, Zhang C, Liu H, Dai Q, Wu L, Lan S, Gopal AV, Trofimov VA, Lysak TM (2012) Selective appearance of several laser-induced periodic surface structure patterns on a metal surface using structural colors produced by femtosecond laser pulses. Appl Surf Sci 258:7625–7632
24. Bonse J, Koter R, Hartelt M, Spaltmanm D, Pentzien S, Höhm S, Rosenfeld A, Krüger J (2014) Femtosecond laser-induced periodic surface structures on steel and titanium alloy for tribological applications. Appl Phys A 117:103–110
25. Hashida M, Semerok AF, Gobert O, Petite G, Izawa Y, Wagner JF (2002) Ablation threshold dependence on pulse duration for copper. Appl Surf Sci 197–198:862–867
26. Bonse J, Munz M, Sturm H (2005) Structure formation on the surface of indium phosphide irradiated by femtosecond laser pulses. J Appl Phys 97:013538
27. Shaheen ME, Gagnon JE, Fryer BJ (2013) Laser ablation of iron: a comparison between femtosecond and picosecond laser pulses. J Appl Phys 114:083110
28. Dufft D, Rosenfeld A, Das SK, Grunwald R, Bonse J (2009) Femtosecond laser-induced periodic surface structures revisited: a comparative study on ZnO. J Appl Phys 105:034908
29. Dar MH, Kuladeep R, Saikiran V, Rao ND (2016) Femtosecond laser nanostructuring of titanium metal towards fabrication of low-reflective surfaces over broad wavelength range. Appl Surf Sci 371:479–487
30. Yoo YE, Kim TH, Choi DS, Hyun SM, Lee HJ, Lee KH, Kim SK, Kim BH, Seo YH, Lee HG, Lee JS (2009) Injection molding of a nanostructured plate and measurement of its surface properties. Curr Appl Phys 9:12–18